

1 Clinical Significance of *TP53*, *BIRC3*, *ATM* and *MAPK-ERK* genes in  
2 Chronic Lymphocytic Leukaemia: Data from the Randomised UK LRF  
3 CLL4 Trial

4 Stuart J. Blakemore<sup>1,9</sup>, Ruth Clifford<sup>2</sup>, Helen Parker<sup>1</sup>, Pavlos Antoniou<sup>2</sup>, Ewa Stec-Dziedzic<sup>2</sup>,  
5 Marta Larrayoz<sup>1</sup>, Zadie Davis<sup>3</sup>, Latha Kadalyayil<sup>4</sup>, Andrew Collins<sup>4</sup>, Pauline Robbe<sup>2</sup>, Dimitris  
6 Vavoulis<sup>2</sup>, Jade Forster<sup>1</sup>, Louise Carr<sup>1</sup>, Ricardo Morilla<sup>5</sup>, Monica Else<sup>5</sup>, Dean Bryant<sup>1</sup>, Helen  
7 McCarthy<sup>3</sup>, Renata J. Walewska<sup>3</sup>, Andrew J. Steele<sup>1</sup>, Jacqueline Chan<sup>6</sup>, Graham Speight<sup>6</sup>,  
8 Tanja Stankovic<sup>7</sup>, Mark S. Cragg<sup>1,8</sup>, Daniel Catovsky<sup>5</sup>, David G. Oscier<sup>3</sup>, Matthew J.J. Rose-  
9 Zerilli<sup>1</sup>, Anna Schuh<sup>2\*</sup>, and Jonathan C. Strefford<sup>1\*</sup>.

10 <sup>1</sup> Academic Unit of Cancer Sciences, Faculty of Medicine, University of Southampton,  
11 Southampton, United Kingdom, <sup>2</sup> Oxford National Institute for Health Research Biomedical  
12 Research Centre and Department of Oncology, University of Oxford, Oxford, United  
13 Kingdom, <sup>3</sup> Department of Molecular Pathology, Royal Bournemouth Hospital,  
14 Bournemouth, United Kingdom, <sup>4</sup> Genetic Epidemiology and Bioinformatics, Faculty of  
15 Medicine, University of Southampton, Southampton, United Kingdom, <sup>5</sup> Division of  
16 Molecular Pathology, The Institute of Cancer Research, London, United Kingdom, <sup>6</sup> Oxford  
17 Gene Technology, Begbroke Science Park, Begbroke, Oxfordshire, United Kingdom.  
18 <sup>7</sup>Institute of Cancer and Genomic Sciences, College of Medical and Dental Services, IBR  
19 West, University of Birmingham, Birmingham, United Kingdom, <sup>8</sup> Antibody & Vaccine Group,  
20 Centre for Cancer Immunology, Cancer Sciences Unit, Faculty of Medicine, University of  
21 Southampton, Southampton General Hospital, Southampton, United Kingdom. <sup>9</sup>  
22 Department I of Internal Medicine, Centre of Excellence in Aging Research, University of  
23 Cologne, Cologne, Germany.

24 \*. These authors contributed equally to the work

25 **Corresponding author:**

26 Jonathan C. Strefford, Cancer Sciences, Faculty of Medicine, University of Southampton,

27 Somers Building, MP824, Tremona Road, Southampton, SO16 6YD, United Kingdom; email:

28 jcs@soton.ac.uk

29 ***Running title:*** *Prognostic impact of recurrently mutated genes in CLL4*

30 **Keywords:** CLL, clinical trial, genetics, mutations, prognosis.

31

32 **Abstract word count: 195**

33 **Main text word count: 3996**

34 **Tables: 2**

35 **Figures: 6**

36

**Abstract**

Despite advances in chronic lymphocytic leukaemia (CLL) treatment, globally chemotherapy remains a central treatment modality, with chemotherapy trials representing an invaluable resource to explore disease-related/genetic features contributing to long-term outcomes. In 499 LRF CLL4 cases, a trial with >12 years follow-up, we employed targeted re-sequencing of 22 genes, identifying 623 mutations. After background mutation rate correction, 11/22 genes were recurrently mutated at frequencies between 3.6% (*NFKB1E*) and 24% (*SF3B1*). Mutations beyond Sanger resolution (<12% VAF) were observed in all genes, with *KRAS* mutations principally composed of these low VAF variants. Firstly, employing orthogonal approaches to confirm <12% VAF *TP53* mutations, we assessed the clinical impact of *TP53* clonal architecture. Whilst  $\geq 12\%$  VAF *TP53*mut cases were associated with reduced PFS and OS, we could not demonstrate a difference between <12% VAF *TP53* mutations and either wild-type or  $\geq 12\%$  VAF *TP53*mut cases. Secondly, we identified biallelic *BIRC3* lesions (mutation and deletion) as an independent marker of inferior PFS and OS. Finally, we observed that mutated *MAPK-ERK* genes were independent markers of poor OS in multivariate survival analysis. In conclusion, our study supports using targeted re-sequencing of expanded gene panels to elucidate the prognostic impact of gene mutations.

## 55 Introduction

56 The application of new technologies continues to reveal the biological basis for the clinical  
57 heterogeneity apparent within CLL<sup>1-3</sup>. In particular, next generation sequencing of large  
58 patient cohorts has led to the discovery of recurring genomic mutations that cluster into  
59 distinct biological signalling pathways. Mutations of specific genes including *TP53*<sup>4-10</sup>,  
60 *ATM*<sup>9,11-14</sup>, *BIRC3*<sup>9,15,16</sup>, *SF3B1*<sup>9,17-20</sup>, *NOTCH1*<sup>1,9,15,17,20-23</sup>, *RPS15*<sup>2,24</sup>, *EGR2*<sup>25,26</sup>, and *KRAS*<sup>27,28</sup>  
61 are associated with poorer outcome, especially shorter time to first treatment or overall  
62 survival (OS). However, numerous factors influence the clinical significance of a driver  
63 mutation in an individual patient. These include clinical status, immunogenetic background,  
64 clone size, the presence of biallelic abnormalities and co-existing driver mutations or copy  
65 number alterations (CNAs). The clinical importance of these potentially confounding factors  
66 is most easily established in context of large clinical trials with long follow-up and where  
67 data on numerous biomarkers are available. One such study is the phase III UK LRF CLL4 trial  
68 (NCT 58585610) that randomly assigned 777 patients to fludarabine (FDR) or fludarabine  
69 plus cyclophosphamide (FC) for six courses, or chlorambucil (CHL) for 12 courses, with the  
70 primary endpoint of overall survival, and secondary endpoints of response rates,  
71 progression-free survival, toxic effects, and quality of life<sup>29</sup>. The trial demonstrated superior  
72 response rates and progression-free survival (PFS) for FC-treated patients compared to  
73 those patients treated with FDR or CHL. Previous genomic analysis of this trial has shown  
74 *TP53*<sup>8</sup>, *SF3B1*<sup>17</sup>, *NOTCH1* (coding<sup>17</sup> and non-coding<sup>21</sup>), *ATM* plus del(11q)<sup>12</sup>, and *EGR2*<sup>26</sup>  
75 lesions to have prognostic significance in multivariate analysis (MVA) and of *RPS15*<sup>24</sup> in  
76 univariate analysis. The importance of data from CLL4 may be questioned given the studies  
77 showing the superior efficacy of FC plus an anti-CD20 antibody (FCR) compared to

78 chemotherapy alone, with the exception of patients with a *NOTCH1* mutation<sup>20</sup>, and  
79 emerging data suggesting the superiority of novel agents compared to chemotherapy-based  
80 regimens. However, the observation that *TP53*, *SF3B1*, and *RPS15* mutations remain poor  
81 risk factors in the German CLL8 trial comparing FCR v FC<sup>20</sup> and the continuing global need  
82 for chemotherapy in CLL for the foreseeable future, indicate that genomic data from the UK  
83 CLL4 trial will continue to have clinical relevance.

84 Accordingly, we performed targeted resequencing on all available pre-treatment samples  
85 (n=499) from the CLL4 trial to investigate the incidence, clinico-biological associations, and  
86 prognostic impact of a panel of 22 genes recurrently mutated in CLL (study overview in  
87 **Figure S1**). Important findings include the failure of <12% VAF *TP53* mutations (1.97 –  
88 11.18% Variant Allele Frequency [VAF]) to influence PFS or OS, the importance of 11q  
89 deletions on PFS and OS in the context of *ATM* and *BIRC3* mutations, and the reduced OS  
90 associated with mutations in the *MAPK-ERK* genes: *BRAF*, *KRAS*, and *NRAS*.

91

## Methods

### *Patients and molecular assays*

We studied 499 patient samples taken at randomization<sup>29</sup>. Patients were diagnosed using the iwCLL guidelines<sup>30</sup>, with informed consent obtained in accordance with the declaration of Helsinki. This study was approved by national/regional research ethics committees. The average lymphocyte percentage of the total white cell count in pre-treatment blood samples was 83.8%. To confirm high tumor load, CD19/CD5 positivity from cases with available flow cytometry data were compared with their matched average lymphocyte percentage (n=233), with an agreement bias of -0.8% (**Figure S2**). Our study cohort did not significantly differ from the entire trial cohort in terms of: treatment allocation, CNAs, age, gender, disease stage, ZAP70/CD38 expression, or IGHV status (**Table S1**). The assessment of established biomarkers was performed as described<sup>31</sup>. All published genetic and biological data on CLL4 patients for genes: *TP53*<sup>8</sup>, *ATM*<sup>12,13</sup>, *BIRC3*<sup>12</sup>, *NOTCH1*<sup>17</sup> (+3'UTR<sup>21</sup>), and *SF3B1*<sup>17</sup>, and CNAs: 13q deletion, 17p deletion, 11q deletion, and trisomy 12 (5%, 10%, 5%, and 3% clone size cut-offs, respectively<sup>31</sup>) were integrated into this study, as well as telomere length<sup>32</sup> and levels of prolymphocytes<sup>33</sup>.

### *Targeted re-sequencing, bioinformatics analysis, variant filtering and validation*

Mutations in 22 genes were analysed in all 499 patients (TruSeq Custom Amplicon, Illumina, San Diego, CA, USA) (**Table S2**). Libraries were generated from 250 ng or 50 ng (dependent on the amount of available starting material) of DNA according to manufacturer's instructions. The average sequencing yield after Illumina processing (MiSeq, paired-end, 2x150 bp) from 28 runs was 6.9Gbp, with a mean read depth of >1000x (range 502 – 7948)

across all targeted genes, with only 9 amplicons below a mean read depth of 1000 (range 502 – 987) (**Figure S3**).

At this depth subclonal mutations can be detected at the 2% level, assuming a minimum observation of 4 sequencing reads containing the variant base, a Q50 phred like base quality score ( $p(\text{detected}) = 99.999$ ) and a cumulative binomial distribution for  $n$  read depth [ $\frac{N!}{n!(N-n)!} p^n (1-p)^{N-n}$ ]. In addition, 6 variants below 2% were included, since the number of sequencing reads in the variant base were more than ten times the assumed minimum observation (range 50 – 126), and the total read depth exceeded 2000 reads in all cases (range 2582 – 6389). Bioinformatic data processing of variants was conducted as previously described<sup>14</sup>.

All mutations included in this study are listed in **Table S3**. As the CLL4 cohort lacked germ-line DNA we only considered variants previously observed as somatically acquired in CLL<sup>1,2,14</sup> or annotated in COSMIC (v70)<sup>34</sup>, except for specific circumstances regarding *TP53*, *ATM*, *BIRC3* and *NOTCH1*. For *TP53*, additional mutations annotated in IARC were re-introduced<sup>35</sup>. Pathogenic *ATM* variants were included if; they were observed in AT families as pathogenic (LOVD [<https://databases.lovd.nl/shared/genes/ATM>]), they were evolutionary rare missense<sup>36</sup>, or were somatically acquired in CLL<sup>13</sup> (**Table S4**). However, this variant strategy does not fully preclude *ATM* variants that exist in germ-line material. For *BIRC3*, only truncating mutations were included<sup>9</sup>. *NOTCH1* PEST domain mutations not predicted to result in protein truncation were removed. All candidate variants were visually inspected in Integrated Genomics Viewer<sup>37</sup>. Genes were defined as recurrent using Tumor Portal ([www.tumorportal.org/power](http://www.tumorportal.org/power)), with the background mutation rate for CLL stated on the website, and the number of cases in the study ( $n = 499$ ) inputted. Mutations were stratified using Sanger sequencing threshold of 12%<sup>5,9</sup>.



Thirty-one percent (194/623) of mutations were validated using orthogonal approaches, including Sanger (n=120) and Ion Torrent (19 low-level *TP53* mutations) sequencing, hybridization-based gene enrichment with subsequent sequencing (n=27) and ddPCR (*SF3B1* p.K700E [n=11], *NOTCH1* p.P2415fs [n=19]). 100% of variants were confirmed using this approach. An excellent agreement between TruSeq and orthogonal-derived VAFs was also observed, with an agreement bias of 0.02% (**Figure S4**).

#### *Statistical analysis*

Fisher's exact tests were performed for co-occurrence analysis between mutated genes and clinical features. PFS and OS was assessed from randomisation using Kaplan Meier (KM) and Log rank analysis. PFS was defined as time from randomisation to progression (i.e. relapse needing further treatment) or death, or to last follow-up date (Oct 2010; final CLL4 PFS update). OS was defined as time from randomisation to death or to last follow-up date for survivors (August 2016, final CLL4 OS update). Multivariate Cox Proportional Hazard models were generated for OS and PFS using backwards selection ( $P < 0.05$ ), to test the confounding effect of multiple prognostic variables. The Bland-Altman test was used to test agreement between multiple factors, reporting the agreement bias, which is the mean difference between two measurements. All reported *P* values were 2-sided and results were considered significant at the 5% level, using multiple hypothesis testing when appropriate (Benjamini and Hochberg method<sup>38</sup>). Statistical analysis was conducted using R v3.3.0, SPSS v23 (IBM), and Prism v6.0g (GraphPad).

## Results

### *Distribution of somatic mutations*

We identified 623 mutations (mean = 1.25, min/max = 0/7 per patient) in 335 patients, 398  $\geq 12\%$  VAF and 225  $< 12\%$  VAF, with 93% of the entire cohort harbouring  $\geq 1$  mutation or CNA (**Figure 1A**). 97 patients without any established CNAs carried 124 mutations (mean = 1.28, min/max = 0/6 per patient), with 22 patients lacking any mutations or CNAs. After background correction (0.5/Mb,  $\geq 3\%$  recurrence, **Table S5**), 11/22 genes were recurrently mutated at frequencies between 3.6% (*NFKBIE*) and 24% (*SF3B1*), (**Figure 1A**, **Table S3**, **Figure S7**). 121 samples harboured 134 *SF3B1* mutations; 46.3% were the p.K700E variant and 30.6% were other hotspot variants (p.K666X, p.H662X, p.G740E, p.G742D). Two or more *SF3B1* mutations were identified in 12 patients (**Figure S5**), with six cases harbouring multiple *SF3B1* mutations present with different VAFs, suggesting the presence of multiple mutated sub-clones. 69 *NOTCH1* mutated patients were identified (13.8%), with 61 mutations in exon 34 (50/61 p.2514fs) and 9 in the 3'UTR. Fifty-five patients carried 59 IARC-annotated *TP53* mutations (exons 4-11, 88% in exons 5-8). Forty pathogenic *ATM* mutations were observed in 37 cases, without evidence of any mutational hotspots. *BIRC3*, *POT*, *BRAF*, *XPO1*, and *KRAS* were mutated in 7.2, 6, 6, 5.8, and 5.8% of cases, respectively. Thirty-eight cases harboured a mutation in *BRAF*, with 7 (18.4%) having the p.V600E variant (**Figure S6**).

*Clinico-biological features of recurrently mutated genes*

Next, we determined statistical associations between these gene mutations, and expansive clinico-biological features, using the Fisher's Exact test (n=1293 tests, **Figure 1B**). 126 associations were observed, including 15 high- (FDR,  $Q > P$  [ $P < 0.05$ ]), 35 medium- ( $P < 0.01$ ), and 76 low-confidence associations ( $P < 0.05$ ). Significant associations between mutations were found in only 10/171 possible associations, such as *NOTCH1*+3'UTR with *BIRC3* ( $P=0.02$ ) and *FBXW7* ( $P=0.01$ ), as well as *BRAF* with *TP53* ( $P=0.03$ ) (**Figure 1B, Table S6**).

*Distribution of  $\geq 12\%$  VAF and  $< 12\%$  VAF mutations*

Next, we classified mutations as Sanger positive ( $\geq 12\%$  VAF) or negative ( $< 12\%$  VAF) by accounting for the impact of tumor purity on VAF. Initially, we studied 233 patients with tumor purity derived from CD5/CD19 flow-cytometry. Raw VAFs were compared with purity-adjusted VAFs across all variants (n=288), including  $< 12\%$  VAFs (n=98), and showed an agreement bias of only 5% (**Figure S8A**), which was even lower for  $< 12\%$  VAF mutations (agreement bias  $< 0.82\%$ , **Figure S8B**). Therefore, we analysed all raw VAFs, and observed three variant populations: those found at  $< 12\%$  VAF (1.49-11.56%, n=225), those at larger sub-clonal or clonal levels (12.06-58.15%, n=356), and those concomitant with deletion events (60.19-99.66%, n=42) (**Figure 2A**). *SAMHD1* mutations were exclusively composed of  $\geq 12\%$  VAF (55.3% mean VAF), while *ATM*, *MYD88*, *NOTCH1*, *SF3B1*, *TP53*, and *XPO1* mutations were found to contain a significant majority of  $\geq 12\%$  VAF mutations. *KRAS* mutations were more likely to be composed of low VAF variants, with a mean VAF of 10.7% (two-way binomial test, False Discovery Rate [FDR],  $Q > P$  [ $P < 0.05$ ]) (**Figure 2B**).

*Univariate impact of mutated genes on PFS and OS*

Clinico-biological features and gene mutations associated with PFS and OS in univariate Cox Proportional Hazards analysis are shown in **Figure 3A**. Gene mutations in *TP53* (with/without del(17p), termed '*TP53ab*') and *EGR2* were associated with reduced PFS (**Figure 3A, Table 1 and Figure S9**). *TP53ab*, and recurrent mutations in *SF3B1*, *NOTCH1* (+3'UTR), *EGR2*, *RPS15*, *NFKBIE*, *BRAF*, *KRAS*, and *NRAS* were associated with reduced OS (**Figure 3A, Table 1 and Figure S10**). As expected, mutations in *MYD88* were confined to IGHV-mutated (IGHV-M) cases, having no significant impact on OS in this subgroup of patients (**Figure S11**). In addition, *TP53* mutations were associated with poor response (**Figure 3B**), *NOTCH1*+3'UTR mutations were associated with death from Richter's syndrome (**Figure 3C**), whilst *TP53*, *SF3B1*, *NOTCH1*+3'UTR, *KRAS*, and *EGR2* were significantly associated with <10yr survival (**Figure 3D**). Other significant associations are included in **Figures S12 & S13**.

*Clinical relevance of TP53 deletions and mutations*

*TP53* mutations below the threshold of Sanger sequencing have been associated with inferior survival in retrospective analysis of institutional cohorts<sup>5,9</sup>. We observed 59 *TP53* mutations in 55 patients (**Figure 4A**); all of those tested (n = 51) were confirmed using orthogonal approaches (**Table S3**). These <12% *TP53* mutated were enriched for *BRAF* and *FBXW7* mutations (**Table S8**). *TP53* mutations could be further subdivided into those with <12% VAF (n = 16) or ≥12% VAF (n = 43), with no difference in the site or type of *TP53* mutation between subgroups (**Figure 4A**). After including 17p FISH data, 58 *TP53ab* patients

were identified, divided into cases with sole 17p deletions (n=3), isolated *TP53* mutations (n=27) or both (n=23). Five *TP53* mutated cases lacked FISH data.

Next, we assessed the genomic complexity of *TP53*mut cases. Both <12% VAF and ≥12% VAF *TP53*mut groups had increased mutation/CNA frequency in comparison to *TP53*wt cases (both  $P<0.001$ ) (**Figure 4B**). To further understand the complexity of these two patient subgroups, we inferred the evolutionary history of *TP53*mut cases as previously described in CLL<sup>2</sup>. Both <12% VAF and ≥12% VAF cases exhibited the same heterogeneous pattern of co-existing mutations, where *TP53* mutations were present at higher, or lower VAFs than concomitant driver mutations (**Table S7, Figure 4C, Figure S14**).

Lastly, we assessed the clinical impact of <12% VAF and ≥12% VAF *TP53*mut subgroups in pairwise Kaplan Meier analysis. ≥12% VAF *TP53*mut were associated with reduced PFS and OS compared to cases with wild-type *TP53* (≥12% *TP53*mut = OS: median = 2.18yrs vs. 6.11yrs,  $P<0.001$ , PFS: median = 0.5yrs vs. 2.17yrs,  $P<0.001$ ). In contrast, we could not demonstrate a significant difference between the <12% VAF *TP53*mut cases and either the wild-type or ≥12% VAF *TP53*mut patients for PFS or OS (<12% *TP53*mut = OS: median = 4.21yrs vs. 6.11yrs,  $P = 0.12$ , PFS: median = 1.92yrs vs. 2.17yrs,  $P = 0.196$ ) (**Figure 4D & 4E**).

These observations held true in 17p deletion stratified analysis (**Figure S15**), confirming the importance of *TP53*mut clone size on survival in this cohort. Stratified <12% VAF vs. ≥12% VAF analysis for other genes with sufficient mutated cases in this cohort can be found in **Figures S16 & S17**.

*Biallelic BIRC3 deleted patients infer reduced overall survival in comparison to sole 11q deleted patients*

Although neither *ATM* nor *BIRC3* mutations, regardless of their VAF (**Figures S16 & S17**), were associated with reduced PFS or OS in univariate survival analysis (**Figures S12 & S13**), it has previously been demonstrated that the impact of these mutations may be dependent on the presence of a concomitant 11q deletion<sup>12,40</sup>. Therefore, we performed an integrated analysis of the clinical impact of *ATM* and *BIRC3* mutations in the context of 11q-deleted CLL. *ATM* Mutations spanned the entire gene, whilst those targeting *BIRC3* were restricted to the CARD domain, as previously shown<sup>9,11–13,40</sup> (**Figure 5A, Figure S7**). Importantly, *ATM* and *BIRC3* mutations were mutually exclusive in our series (**Figure 5B**), suggesting that these mutations may define sub-groups of 11q-deleted CLL. Deletions of 11q were identified using a FISH probe which encompasses the *ATM* but not the *BIRC3* locus. Accordingly, concomitant *BIRC3* loss was defined from previously published SNP6.0 data<sup>12</sup>, or where additional DNA was available (n=21), using shallow WGS (positive cases presented in **Figure S18**). Cases (n= 135) were then categorised into five distinct subgroups: sole 11q deletion (n = 71), biallelic *ATM* abnormalities (abs) (n = 12), biallelic *BIRC3* abs (n = 9), sole *ATM* mutations (n = 24) and sole *BIRC3* mutations (n = 19).

After omitting 10 cases with co-existing *TP53ab*<sup>12</sup>, we conducted pairwise KM analysis for these five groups compared to cases with no 11q abnormality. (**Figure 5C and 5D; Figure S19**). For both PFS and OS, sole 11q deletion (PFS: median = 1.4yrs vs. 2.5yrs,  $P<0.0001$ , OS: median = 4.8yrs vs. 6.4yrs,  $P=0.002$ ), as well as biallelic *ATM* (PFS: median = 1yr vs. 2.5yrs,  $P=0.001$ , OS: median = 4.2yrs vs. 6.4yrs,  $P=0.049$ ) and biallelic *BIRC3* (PFS: median = 1yr vs.

2.5yrs,  $P < 0.0001$ , OS: median = 3.3yrs vs. 6.4yrs,  $P = 0.001$ ), were associated with a significantly reduced survival.

The outcome of cases with biallelic abs was then compared to those with del(11q) only.

There were no significant differences in PFS (biallelic *ATM* vs. 11q = 1yr vs. 1.4yrs,  $P = 0.336$ ; biallelic *BIRC3*: 1yr vs. 1.4yrs,  $P = 0.178$ ); however cases with biallelic *BIRC3* abs had a significantly reduced OS, whilst cases with biallelic *ATM* abs did not significantly differ in median survival times compared to sole 11q deleted cases (biallelic *ATM* vs. 11q = 4.2yrs vs. 4.8yrs,  $P = 0.493$ ; biallelic *BIRC3*: 3.3yrs vs. 4.8yrs,  $P = 0.03$ ). This suggests that biallelic loss of *BIRC3* represents the subgroup of 11q deleted CLL with the worst outcome following initial treatment with chemotherapy.

*MAPK-ERK pathway members: BRAF, KRAS, and NRAS, all infer poor overall survival in CLL4*

Mutations in *MAPK-ERK* genes, *BRAF* (38 mutations/30 cases), *KRAS* (34/29) and *NRAS* (11/10), were principally composed of specific hotspot variants (*BRAF*: p.G469A/E, *KRAS*: p.G13D, *NRAS*: p.Q61K/R) (**Figure S7**), and the majority of *MAPK-ERK* mutated cases (87%) only harboured a mutation in one of these genes (**Figure 6A**). Interestingly, *MAPK-ERK* mutated patients displayed an increased frequency of mutated genes and CNVs per case versus *MAPK-ERK* wild-type patients (**Figure S20**). In univariate analysis, each mutation was associated with a shorter median OS than wildtype: *BRAF* (OS median: 3.92yrs vs. 6yrs,  $P = 0.009$ ), *KRAS* (OS median: 3.83yrs vs. 5.89yrs,  $P < 0.001$ ), and *NRAS* (OS median: 4.24yrs vs. 5.88yrs,  $P = 0.01$ ) (**Figure 6B-D**). Stratified  $<12\%$  VAF vs.  $\geq 12\%$  VAF analysis indicated that the outcome of *KRAS* mutated cases was independent of VAF while shorter OS in *BRAF* mutated cases was associated with  $<12\%$  VAF (**Figure S16; Table S9**). Taken together,

*MAPK-ERK* mutations exhibited inferior OS compared to wildtype cases (OS median: 3.83yrs vs. 6.10yrs,  $P < 0.001$ ), and were negatively associated with long-term survival (Odds Ratio = 0.19,  $P = 0.0003$ ) (**Figure 6E**), with only 4/60 mutated cases defined as long-term survivors. Furthermore, *MAPK-ERK* mutated patients were more likely to carry IGHV-U genes (IGHV-U Odds Ratio = 4.29,  $P < 0.0001$ ; IGHV homology >99% Odds Ratio = 3.51,  $P = 0.0002$ ), and significantly less likely to harbour del(13q) as a sole aberration (Odds Ratio = 0.23,  $P < 0.0001$ , **Table S10**).

*Multivariate modelling identifies TP53ab, biallelic BIRC3, SF3B1, EGR2, and MAPK-ERK gene mutations as independent markers of inferior OS.*

Finally, we constructed comprehensive multivariate Cox Proportional Hazards models for PFS and OS (**Table 2**) which included those clinical and genetic variables significant in univariate analysis, as well as biallelic *ATM* and *BIRC3* they emerged from our stratified 11q deletion analysis, and short telomeres based on our previous paper on the topic<sup>32</sup>. A backwards selection approach was applied, until all variables within the model had a  $P$  value  $< 0.05$ . For PFS, the final model was constructed from 225 patients and 210 events (274 were excluded due to missing data) and showed that *TP53ab* (HR = 4.98,  $P < 0.001$ ), biallelic *BIRC3* (HR = 3.83,  $P = 0.004$ ), short telomeres (HR = 1.96,  $P < 0.001$ ), sole 11q deletion (HR = 1.82,  $P = 0.003$ ), and increased prolymphocytes (HR = 1.51,  $P = 0.033$ ) were independent markers of PFS. For OS, the final model was constructed from 391 patients and 323 events (108 observations were excluded due to missing data). *TP53ab* (HR = 4.25,  $P < 0.001$ ), biallelic *BIRC3* (HR = 2.76,  $P = 0.004$ ), mutations in *EGR2* (HR = 2.19,  $P = 0.015$ ), *MAPK-ERK* genes (HR = 1.68,  $P = 0.002$ ), *SF3B1* (HR = 1.54,  $P = 0.001$ ), as well as IGHV-U genes (HR = 1.83,  $P < 0.001$ ) and Binet stage B&C (HR = 1.45,  $P = 0.008$ ), were all observed as independent



markers of OS. This data confirms our univariate survival analysis, showing that cases with biallelic *BIRC3* deletions exhibit reduced PFS and OS, and that mutations in the *MAPK-ERK* pathway lead to reduced OS.

## Discussion

We report targeted re-sequencing analysis of 22 genes known to be recurrently mutated in CLL in the UK CLL4 clinical trial. CLL4 represents an ideal candidate for such an analysis, with expansive clinical and biological description<sup>8,12,33, 13,17,21,24,26,29,31,32,41,42</sup> and protracted clinical follow-up. Our study confirms previous studies incorporating samples from this patient cohort showing the impact of *TP53*ab on PFS and OS in MVA, *SF3B1*, *EGR2*<sup>25,26</sup>, *RPS15*<sup>1,24</sup> and *NFKB1E*<sup>25,28,43</sup> mutations on OS in univariate analysis, with *SF3B1* and *EGR2* mutations retained as independent markers of OS in multivariate analysis.

The literature suggests that patients with *MAPK-ERK* mutations represent a biologically distinct subgroup, where *MAPK-ERK* mutations are frequently mutually exclusive, are enriched for trisomy 12, unmutated IGHV genes and other adverse biological markers (e.g. CD38, ZAP-70, CD49d), and are linked to inferior time to first treatment in retrospective cohorts<sup>42,44–46</sup>. We now show the *MAPK-ERK* genes, *BRAF*, *KRAS*, and *NRAS* (collectively representing 12.2% of patients) are also independently associated with short OS in a cohort of patients requiring treatment. Vendramini *et al.* showed a similar frequency of mutations in these genes (14%)<sup>45</sup>, while Giménez and co-workers found that 5.5% of CLL cases harbours functionally deleterious mutations in 11 genes involved in the *MAPK-ERK* pathway<sup>46</sup>, the latter likely reflects the early-stage composition of the cohort. In support of the biological impact of these mutated genes in CLL, 1) Analysis of mutated patients exhibit an enrichment of gene sets associated with transcriptional activation of the *MAPK-ERK*

pathway<sup>45</sup>, 2) preliminary *in vitro* analysis suggests cells from these patients are prone to killing with ERK inhibitors<sup>46</sup>, 3) *BRAF* mutations accelerated disease progression in Eμ-TCL1 mice<sup>47</sup>, 4) mutant *BRAF* has been implicated in venetoclax resistance<sup>48</sup>, and 5) *KRAS* mutated cases associated with poor response to chemoimmunotherapy<sup>27</sup> and lenalidomide<sup>49</sup>.

Screening for *TP53*ab using FISH and Sanger sequencing has known prognostic value<sup>6,8,20,31</sup>, and predicts for resistance to chemo-immunotherapy<sup>50</sup>. *TP53* mutations that present at low VAFs, below the detection limit of conventional Sanger sequencing may also be positively selected by chemotherapy, and also predict inferior survival, at least in retrospective, institutional cohorts<sup>3,5,9</sup>. The *TP53* Network of ERIC provide expansive guidelines on the most suitable approach for *TP53* mutational analysis, but also conclude that the clinical importance of low-level *TP53* clones remains an unresolved issue, requiring validation in clinical trials<sup>50</sup>. We demonstrated inferior PFS and OS only for those patients with  $\geq 12\%$  VAF *TP53* mutations, but we could not demonstrate inferior survival associated with cases harboring  $<12\%$  VAF *TP53* mutations, the inference perhaps is that these cases represent an intermediate-risk group. Given the unexpected nature of this finding, we also conducted stratified 17p deleted survival analysis, identifying the same result for  $<12\%$  VAF *TP53* mutations without 17p deletion. Furthermore, we proceeded to show that our observation was not associated with any differences in the type of *TP53* mutation, their co-existence with other more clonal prognostically-important gene mutations or biological features, nor the enrichment of any specific treatment. As a consequence, we feel that our observation is technically sound, and warrants confirmation in further studies.

There remains disagreement regarding the relative clinical significance of deletion and mutation of the *BIRC3* and *ATM* genes, both mapping to the long arm of chromosome 11.

The *ATM* gene is mutated in 30-40% of 11q deleted patients<sup>11,13</sup>, where it results in biallelic inactivation of *ATM*, driving an impaired DNA damage response<sup>51</sup>. The prognostic impact of *ATM* mutations is controversial in unselected cohorts<sup>9</sup>, with the strongest impact when the wild-type allele is lost. In our study, whilst we triaged *ATM* mutations based on their putative pathogenicity, several are reported in both somatic (i.e. COSMIC) and germline (i.e. dbSNP, EXAC, ClinVar) databases, lending uncertainty to their prognostic impact. The sequencing of matched germ-line material would provide additional clarity, but was not possible due to the historical nature of CLL4. Preliminary studies support a pathogenetic role of *BIRC3*<sup>16,40</sup>, more recent studies provide less certainty. For example, in the RESONATE clinical trial<sup>52</sup> and the large retrospective study coordinated by ERIC<sup>53</sup>, *BIRC3* mutations were not linked to inferior PFS or TTFT, respectively. Another comparator would be the RESONATE2 trial, which compared first line treatment with Ibrutinib v chlorambucil<sup>54</sup>. The 24 month PFS for 11q deleted patients in the Ibrutinib arm was 97%. Further studies are required to determine if the long-term outcome of biallelic *BIRC3* cases is equally good under modern small molecule inhibition. In our previous CLL4 analysis, we demonstrated that *BIRC3* dysfunction (defined as deletion AND/OR mutations of *BIRC3*) did not impact survival in 11q deleted CLL, while biallelic *ATM* lesions remained informative<sup>12</sup>. However, this analysis utilized Sanger sequencing, and hence only identified a small number of *BIRC3* mutations. Our current study, therefore aimed to expand the analysis with a larger patient cohort with significantly improved technology. This approach permitted the identification of a meaningful number of cases with loss and mutation of *BIRC3*. As neither *ATM* nor *BIRC3* mutations were linked to survival in univariate analysis, we performed a stratified analysis in 11q-deleted cases. In so doing, we show that biallelic *BIRC3* cases have a further reduction in survival in comparison to sole 11q deleted cases and were found to be independent

prognostic markers for PFS and OS in MVA. Finally, *ATM* and *BIRC3* mutated cases without 11q deletion have a similar survival to wildtype cases.

In conclusion, our study makes three main contributions to the field. We show an expansive analysis of the impact of clinico-biological disease features on the clinical importance of important gene mutations, including *SF3B1*, *EGR2*, and the *MAPK-ERK* genes. Our analysis suggests that <12% VAF *TP53* mutations are an intermediate survival group. Finally, we show that biallelic *BIRC3* aberrations identify a novel patient subgroup with poor survival, inferior to those with 11q-deletions alone. Taken together, we demonstrate that a more expansive genomic screening approach provides additional clinical information, thereby helping to establish the precise importance of genetic alterations in the context of other established and emerging biomarkers. Furthermore, our work will facilitate the development of international standards for the detection and interpretation of somatic mutations in CLL.

## Declaration of interests

The authors declare no conflict of interest.

## Acknowledgements

The authors would like to gratefully acknowledge all the patients and clinicians than contributed to the UK CLL4 trial. The CLL4 trial was funded by a core grant from Bloodwise. ME was supported by the Arbib Charitable Fund. This study was supported by grants and from Bloodwise (12036, 11052), Kay Kendall Leukaemia Fund (873), Cancer Research UK (C2750/A23669, C34999/A18087, ECMC C24563/A15581) and the Oxford Partnership Comprehensive Biomedical Research Centre with funding from the Department of Health's

National Institute of Health Research (NIHR) Biomedical Research Centre funding scheme. The views expressed in this publication are those of the authors and not necessarily those of the Department of Health. Thank you to Miss Kate Latham for contributing to DNA extraction of CLL4 patient samples.

## Author contributions

SJB, MJJR-Z, RC, AS, and JCS designed the research. SJB, MJJR-Z & JCS analysed the data. SJB, MJJR-Z, DGO & JCS and wrote the paper. SJB, RC, HP, PA, ES-D. ML, ZD, LK PR, DV, JF, AB, RM, DC, ME, DB, HMC, DGO, RJW, AIS, MSC, MJJRZ, and AS performed the research and/or contributed patient samples and associated data. All authors read and agreed to the final version of the manuscript.

## References

1. Puente, X. S., Beà, S., Valdés-Mas, R., Villamor, N., Gutiérrez-Abril, J., Martín-Subero, J. I., *et al.* Non-coding recurrent mutations in chronic lymphocytic leukaemia. *Nature* **526**, 519–524 (2015).
2. Landau, D. A., Tausch, E., Taylor-weiner, A. N., Stewart, C., Reiter, J. G., Bahlo, J., *et al.* Mutations driving CLL and their evolution in progression and relapse. **526**, 525–530 (2015).
3. Nadeu, F., Martín-García, D., López-Guillermo, A., Navarro, A., Colado, E., Campo, E., *et al.* Clinical impact of the subclonal architecture and mutational complexity in chronic lymphocytic leukemia. *Leukemia* **32**, 645–653 (2017).
4. Minervini, C. F., Cumbo, C., Orsini, P., Brunetti, C., Anelli, L., Zagaria, A., *et al.* TP53 gene mutation analysis in chronic lymphocytic leukemia by nanopore MinION sequencing. *Diagn. Pathol.* **11**, 96 (2016).
5. Rossi, D., Khiabani, H., Spina, V., Ciardullo, C., Brusca, A., Famà, R., *et al.* Clinical impact of small TP53 mutated subclones in chronic lymphocytic leukemia. *Blood* **123**, 2139–2148 (2014).
6. Zenz, T., Eichhorst, B., Busch, R., Denzel, T., Habe, S., Winkler, D., *et al.* TP53 Mutation and Survival in Chronic Lymphocytic Leukemia. *J. Clin. Oncol.* **28**, 4473–4479 (2010).
7. Malcikova, J., Stano-Kozubik, K., Tichy, B., Kantorova, B., Pavlova, S., Tom, N., *et al.* Detailed analysis of therapy-driven clonal evolution of TP53 mutations in chronic lymphocytic leukemia. *Leukemia* **29**, 877–85 (2015).
8. Gonzalez, D., Martinez, P., Wade, R., Hockley, S., Oscier, D., Matutes, E., *et al.* Mutational Status of the TP53 Gene As a Predictor of Response and Survival in Patients With Chronic Lymphocytic Leukemia: Results From the LRF CLL4 Trial. *J. Clin. Oncol.* **29**, 2223–2229 (2011).
9. Nadeu, F., Delgado, J., Royo, C., Baumann, T., Stankovic, T., Pinyol, M., *et al.* Clinical impact of clonal and subclonal TP53, SF3B1, BIRC3, NOTCH1 and ATM mutations in chronic lymphocytic leukemia. *Blood* **127**, 2122–2130 (2016).
10. Pekova, S., Mazal, O., Cmejla, R., Hardekopf, D. W., Plachy, R., Zejskova, L., *et al.* A comprehensive study of TP53

- 431 mutations in chronic lymphocytic leukemia: Analysis of 1287 diagnostic and 1148 follow-up CLL samples. *Leuk.*  
 432 *Res.* **35**, 889–898 (2011).
- 433 11. Austen, B., Powell, J. E., Alvi, A., Edwards, I., Hooper, L., Starczynski, J., *et al.* Mutations in the ATM gene lead to  
 434 impaired overall and treatment-free survival that is independent of IGVH mutation status in patients with B-CLL.  
 435 *Blood* **106**, 3175–3182 (2005).
- 436 12. Rose-Zerilli, M. J. J., Forster, J., Parker, H., Parker, A., Rodri, A. É., Chaplin, T., *et al.* ATM mutation rather than  
 437 BIRC3 deletion and/or mutation predicts reduced survival in 11q-deleted chronic lymphocytic leukemia: Data from  
 438 the UK LRF CLL4 trial. *Haematologica* **99**, 736–742 (2014).
- 439 13. Skowronska, A., Parker, A., Ahmed, G., Oldreive, C., Davis, Z., Richards, S., *et al.* Biallelic ATM inactivation  
 440 significantly reduces survival in patients treated on the United Kingdom leukemia research fund chronic  
 441 lymphocytic leukemia 4 trial. *J. Clin. Oncol.* **30**, 4524–4532 (2012).
- 442 14. Guièze, R., Robbe, P., Clifford, R., De Guibert, S., Pereira, B., Timbs, A., *et al.* Presence of multiple recurrent  
 443 mutations confers poor trial outcome of relapsed/refractory CLL. *Blood* **126**, 2110–2117 (2015).
- 444 15. Fabbri, G., Rasi, S., Rossi, D., Trifonov, V., Khiabani, H., Ma, J., *et al.* Analysis of the chronic lymphocytic leukemia  
 445 coding genome: role of NOTCH1 mutational activation. *J. Exp. Med.* **208**, 1389–401 (2011).
- 446 16. Rossi, D., Rasi, S., Spina, V., Bruscaggini, A., Monti, S., Ciardullo, C., *et al.* Integrated mutational and cytogenetic  
 447 analysis identifies new prognostic subgroups in chronic lymphocytic leukemia. **121**, 1403–1412 (2013).
- 448 17. Oscier, D. G., Rose-Zerilli, M. J. J., Winkelmann, N., Gonzalez de Castro, D., Gomez, B., Forster, J., *et al.* The clinical  
 449 significance of NOTCH1 and SF3B1 mutations in the UK LRF CLL4 trial. *Blood* **121**, 468–475 (2012).
- 450 18. Jeromin, S., Weissmann, S., Haferlach, C., Dicker, F., Bayer, K., Grossmann, V., *et al.* SF3B1 mutations correlated to  
 451 cytogenetics and mutations in NOTCH1, FBXW7, MYD88, XPO1 and TP53 in 1160 untreated CLL patients. *Leukemia*  
 452 **28**, 108–117 (2014).
- 453 19. Quesada, V., Conde, L., Villamor, N., Ordóñez, G. R., Jares, P., Bassaganyas, L., *et al.* Exome sequencing identifies  
 454 recurrent mutations of the splicing factor SF3B1 gene in chronic lymphocytic leukemia. *Nat. Genet.* **44**, 47–52  
 455 (2012).
- 456 20. Stilgenbauer, S., Schnaiter, A., Paschka, P., Zenz, T., Rossi, M., Döhner, K., *et al.* Gene mutations and treatment  
 457 outcome in chronic lymphocytic leukemia: Results from the CLL8 trial. *Blood* **123**, 3247–3254 (2014).
- 458 21. Larrayoz, M., Rose-Zerilli, M. J. J., Kadalayil, L., Parker, H., Blakemore, S., Forster, J., *et al.* Non-coding NOTCH1  
 459 mutations in chronic lymphocytic leukemia; their clinical impact in the UK CLL4 trial. *Leukemia* **31**, 510–514 (2016).
- 460 22. Rossi, D., Rasi, S., Fabbri, G., Spina, V., Fangazio, M., Forconi, F., *et al.* Mutations of NOTCH1 are an independent  
 461 predictor of survival in chronic lymphocytic leukemia. *Blood* **119**, 521–529 (2016).
- 462 23. Puente, X. S., Pinyol, M., Quesada, V., Conde, L., Ordóñez, G. R., Villamor, N., *et al.* Whole-genome sequencing  
 463 identifies recurrent mutations in chronic lymphocytic leukaemia. *Nature* **475**, 101–105 (2011).
- 464 24. Ljungstrom, V., Cortese, D., Young, E., Pandzic, T., Mansouri, L., Plevova, K., *et al.* Whole expme sequencing in  
 465 relapsig chronic lymphocytic leukemia: clinical impact of recurrent RPS15 mutations. *Blood* **127**, 1007–1016  
 466 (2016).
- 467 25. Damm, F., Mylonas, E., Cosson, A., Yoshida, K., Della Valle, V., Mouly, E., *et al.* Acquired initiating mutations in  
 468 early hematopoietic cells of CLL patients. *Cancer Discov.* **4**, 1088–1101 (2014).
- 469 26. Young, E., Noerenberg, D., Mansouri, L., Ljungström, V., Frick, M., Sutton, L.-A., *et al.* EGR2 mutations define a new  
 470 clinically aggressive subgroup of chronic lymphocytic leukemia. *Leukemia* **31**, 1547–1554 (2017).
- 471 27. Herling, C. D., Klaum??nzer, M., Rocha, C. K., Altm??ller, J., Thiele, H., Bahlo, J., *et al.* Complex karyotypes and  
 472 KRAS and POT1 mutations impact outcome in CLL after chlorambucil-based chemotherapy or

- chemoimmunotherapy. *Blood* **128**, 395–404 (2016).
28. Doménech, E., Gómez-López, G., Gzlez-Peña, D., López, M., Herreros, B., Menezes, J., *et al.* New mutations in chronic lymphocytic leukemia identified by target enrichment and deep sequencing. *PLoS One* **7**, 2–7 (2012).
  29. Catovsky, D., Richards, S., Matutes, E., Oscier, D., Dyer, M., Bezares, R., *et al.* Assessment of fludarabine plus cyclophosphamide for patients with chronic lymphocytic leukaemia (the LRF CLL4 Trial): a randomised controlled trial. *Lancet* **370**, 230–239 (2007).
  30. Hallek, M., Cheson, B. D., Catovsky, D., Caligaris-Cappio, F., Dighiero, G., Döhner, H., *et al.* Guidelines for the diagnosis and treatment of chronic lymphocytic leukemia: a report from the International Workshop on Chronic Lymphocytic Leukemia updating the National Cancer Institute-Working Group 1996 guidelines. *Blood* **111**, 5446–56 (2008).
  31. Oscier, D., Wade, R., Davis, Z., Morilla, A., Best, G., Richards, S., *et al.* Prognostic factors identified three risk groups in the LRF CLL4 trial, independent of treatment allocation. *Haematologica* **95**, 1705–1712 (2010).
  32. Strefford, J. C., Kadalayil, L., Forster, J., Rose-Zerilli, M. J. J., Parker, A., Lin, T. T., *et al.* Telomere length predicts progression and overall survival in chronic lymphocytic leukemia: Data from the UK LRF CLL4 trial. *Leukemia* **29**, 2411–2414 (2015).
  33. Oscier, D., Else, M., Matutes, E., Morilla, R., Strefford, J. C. & Catovsky, D. The morphology of CLL revisited: the clinical significance of prolymphocytes and correlations with prognostic/molecular markers in the LRF CLL4 trial. *Br. J. Haematol.* **174**, 767–775 (2016).
  34. Forbes, S. A., Beare, D., Boutselakis, H., Bamford, S., Bindal, N., Tate, J., *et al.* COSMIC: somatic cancer genetics at high-resolution. *Nucleic Acids Res.* **45**, D777–D783 (2017).
  35. Petitjean, A., Mathe, E., Kato, S., Ishioka, C., Tavtigian, S., Hainaut, P., *et al.* Impact of Mutant p53 Functional Properties on TP53 Mutation Patterns and Tumor Phenotype: Lessons from Recent Developments in the IARC TP53 Database. *Hum. Mutat.* **28**, 622–629 (2007).
  36. Tavtigian, S. V., Oefner, P. J., Babikyan, D., Hartmann, A., Healey, S., Calvez-kelm, F. Le, *et al.* Rare , Evolutionarily Unlikely Missense Substitutions in ATM Confer Increased Risk of Breast Cancer. *Am. J. Hum. Genet.* **85**, 427–446 (2009).
  37. Robinson, J. T., Thorvaldsdottir, H., Winckler, W., Guttman, M., Lander, E. S., Getz, G., *et al.* Integrated Genomics Viewer. *Nat Biotechnol* **29**, 24–26 (2011).
  38. Benjamini, Y. & Hochberg, Y. Controlling the False Discovery Rate : A Practical and Powerful Approach to Multiple Testing. *J. R. Stat. Soc.* **57**, 289–300 (1995).
  39. Lawrence, M. S., Stojanov, P., Mermel, C. H., Robinson, J. T., Garraway, L. a, Golub, T. R., *et al.* Discovery and saturation analysis of cancer genes across 21 tumour types. *Nature* **505**, 495–501 (2014).
  40. Rossi, D., Fangazio, M., Rasi, S., Vaisitti, T., Monti, S., Cresta, S., *et al.* Disruption of BIRC3 associates with fludarabine chemorefractoriness in TP53 wild-type chronic lymphocytic leukemia. *Blood* **119**, 2854–2862 (2012).
  41. Parker, H., Rose-Zerilli, M. J. J., Larrayoz, M., Clifford, R., Edelmann, J., Blakemore, S., *et al.* Genomic disruption of the histone methyltransferase SETD2 in chronic lymphocytic leukaemia. *Leukemia* **30**, 2179–2186 (2016).
  42. Pandzic, T., Larsson, J., He, L., Kundu, S., Ban, K., Akhtar-Ali, M., *et al.* Transposon Mutagenesis Reveals Fludarabine Resistance Mechanisms in Chronic Lymphocytic Leukemia. *Clin. Cancer Res.* **22**, 6217–6227 (2016).
  43. Mansouri, L., Sutton, L.-A., Ljungström, V., Bondza, S., Arngården, L., Bhoi, S., *et al.* Functional loss of IκBε leads to NF-κB deregulation in aggressive chronic lymphocytic leukemia. *J. Exp. Med.* **212**, 833–843 (2015).
  44. Leeksa, A. C., Taylor, J., Dubois, J., Dietrich, S., de Boer, F., Zelenetz, A., *et al.* Clonal diversity predicts adverse outcome in chronic lymphocytic leukemia. *Leukemia* **33**, 390–402 (2018).

45. Vendramini, E., Bomben, R., Pozzo, F., Benedetti, D., Bittolo, T., Rossi, F. M., *et al.* KRAS, NRAS, and BRAF mutations are highly enriched in trisomy 12 chronic lymphocytic leukemia and are associated with shorter treatment-free survival. *Leukemia* **12**, 10–14 (2019).
46. Giménez, N., Valero, J. G., López-Otín, C., Payer, A. R., Puente, X. S., Martínez-Trillos, A., *et al.* Mutations in RAS-BRAF-MAPK-ERK pathway define a specific subgroup of patients with adverse clinical features and provide new therapeutic options in chronic lymphocytic leukemia. *Haematologica* **104**, 576–586 (2018).
47. Tsai, Y.-T., Sass, E. J., Lozanski, G., Byrd, J. C., Harrington, B. K., Jaynes, F., *et al.* BRAF V600E accelerates disease progression and enhances immune suppression in a mouse model of B-cell leukemia. *Blood Adv.* **1**, 2147–2160 (2017).
48. Herling, C. D., Abedpour, N., Weiss, J., Schmitt, A., Jachimowicz, R. D., Merkel, O., *et al.* Clonal dynamics towards the development of venetoclax resistance in chronic lymphocytic leukemia. *Nat. Commun.* **9**, 727 (2018).
49. Takahashi, K., Wierda, W. G., Keating, M., Kim, E., Thompson, P., Burger, J. A., *et al.* Clinical implications of cancer gene mutations in patients with chronic lymphocytic leukemia treated with lenalidomide. *Blood* **131**, 1820–1832 (2018).
50. Malcikova, J., Tausch, E., Rossi, D., Sutton, L. A., Soussi, T., Zenz, T., *et al.* ERIC recommendations for TP53 mutation analysis in chronic lymphocytic leukemia - Update on methodological approaches and results interpretation. *Leukemia* **32**, 1070–1080 (2018).
51. Austen, B., Skowronska, A., Baker, C., Powell, J. E., Gardiner, A., Oscier, D., *et al.* Mutation status of the residual ATM allele is an important determinant of the cellular response to chemotherapy and survival in patients with chronic lymphocytic leukemia containing an 11q deletion. *J. Clin. Oncol.* **25**, 5448–5457 (2007).
52. Brown, J. R., Delgado, J., Jaeger, U., Montillo, M., Hillmen, P., Kipps, T. J., *et al.* Extended follow-up and impact of high-risk prognostic factors from the phase 3 RESONATE study in patients with previously treated CLL/SLL. *Leukemia* **32**, 83–91 (2017).
53. Baliakas, P., Hadzidimitriou, A., Sutton, L. A., Rossi, D., Minga, E., Villamor, N., *et al.* Recurrent mutations refine prognosis in chronic lymphocytic leukemia. *Leukemia* **29**, 329–336 (2015).
54. Barr, P. M., Robak, T., Owen, C., Tedeschi, A., Bairey, O., Bartlett, N. L., *et al.* Sustained efficacy and detailed clinical follow-up of first-line ibrutinib treatment in older patients with chronic lymphocytic leukemia: extended phase 3 results from RESONATE-2. *Haematologica* **103**, (2018).



## Figure Legends

### Figure 1. Mutation landscape and co-occurrence associations of the CLL4 cohort.

**A** Mutational Landscape of CLL4. In the Waterfall plot, known recurrently mutated genes and copy number alterations are shown, hierarchically clustered by mutation frequency (vertical bar chart, right). The mutation burden captured by the study is shown in the bar chart above the heat map. Mutation types are depicted in the above key. The inset vertical bar chart represents the distribution of the number of mutated genes/CNAs per case. **B** Co-occurrence of all available clinico-biological features from the CLL4 clinical trial. The co-occurrence (red) or mutual exclusivity (green) is plotted per interaction in the graph based on the level of significance (from light to dark:  $P < 0.05$ ,  $P < 0.01$ ,  $Q > P$  [ $P < 0.05$ ],  $Q > P$  [ $P < 0.01$ ]).

### Figure 2. CLL4 mutation architecture.

**A** Distribution of mutation variant allele frequency. Scatter plot of all variants by read depth and VAF (red dots =  $< 12\%$  VAF [left of dotted line], blue dots =  $> 12\%$  VAF). **B** Distribution of  $\geq 12\%$  and  $< 12\%$  variants. Top: Proportion of  $\geq 12\%$  and  $< 12\%$  variants ranked by highest proportion of  $\geq 12\%$  VAF variants. Two-way binomial distribution used to test whether genes contained significantly more  $\geq 12\%$  VAF or  $< 12\%$  VAF mutations, with asterisks representing genes which retained significance after multiple hypothesis testing ( $Q > P$  [ $P < 0.05$ ]). Bottom: VAF distribution of variants per gene. Variants with loss of the other allele (identified by FISH), shown in red for biallelic *TP53*, turquoise for biallelic *ATM* and pink for biallelic *BIRC3*.

### Figure 3. Clinical outcome of mutated genes, CNAs, and clinical features in CLL4.

**A** Forest plot showing the hazard ratios of 26 significant variables for either overall survival (left; black) or progression free survival (right; red) in univariate survival analysis. Variables sorted by the hazard ratio values for overall survival. **B** Bar chart showing the mutation frequency difference between *TP53*mut cases who achieved CR/NodPR or NR/PD. **C** Bar chart showing the *NOTCH1*+3'UTR mutation frequency in relation to Death from Richter's syndrome. **D** Bar chart showing the mutation frequency in relation to patients termed 'long-term survivors' for *TP53*, *SF3B1*, *NOTCH*+3'UTR, *KRAS*, and *EGR2*.

**Figure 4. Clinical relevance of <12% VAF *TP53* mutations in CLL4.**

**A** Mutation Lollipop displaying the *TP53* mutations observed in CLL4, stratified by Sanger sequencing threshold. **B** Mutated genes/CNVs per *TP53*mut subgroup. One-way ANOVA conducted vs. *TP53*wt cases. **C** Examples of In-going and out-going edges drawn from each *TP53*mut subgroup, with patient ID number and IGHV status defined above each graph. **D** OS pairwise KM plot comparing  $\geq 12\%$  VAF *TP53*mut cases (red),  $< 12\%$  VAF *TP53*mut cases (green), and *TP53*wt cases (black). **E** PFS pairwise KM plot comparing  $\geq 12\%$  VAF *TP53*mut cases (red),  $< 12\%$  VAF *TP53*mut cases (green), and *TP53*wt cases (black). Inset table in D&E displays pairwise log rank *P* values between each variable vs. wild type.

**Figure 5. Importance of 11q deletion in the context of *ATM* and *BIRC3* mutations in CLL4.**

**A** Mutation Lollipop of *ATM* (upper) and *BIRC3* (lower) mutations observed in CLL4. **B** Heat map of *ATM* and *BIRC3* mutated cases stratified by 11q deletion status. **C** OS pairwise KM plot comparing mutated *ATM* (left) and *BIRC3* (right) in the context of 11q deletion. **D** PFS pairwise KM plot comparing mutated *ATM* (left) and *BIRC3* (right) in the context of 11q deletion. Inset table in C&D displays pairwise log rank *P* values between each variable vs.

591 wild type for combined pairwise KM analysis of *ATM* and *BIRC3* in the context of 11q  
592 deletion.

593

594 **Figure 6. *MAPK-ERK* genes predict poor OS in CLL4.**

595 **A** Heat map of *BRAF* (blue), *KRAS* (green), *NRAS* (red), and co-mutated genes of *MAPK-ERK*  
596 mutated cases (black). Cases wildtype for each gene represented by grey bars. **B-E** Overall  
597 survival univariate KM plots for *BRAF* (**B**), *KRAS* (**C**), *NRAS* (**D**), and a combined variable of  
598 *APK-ERK* (**E**). Coloured line represents mutated cases, black line represents wild type cases.

**Table 1. Univariate survival association analysis for overall survival and progression free survival in CLL4.**

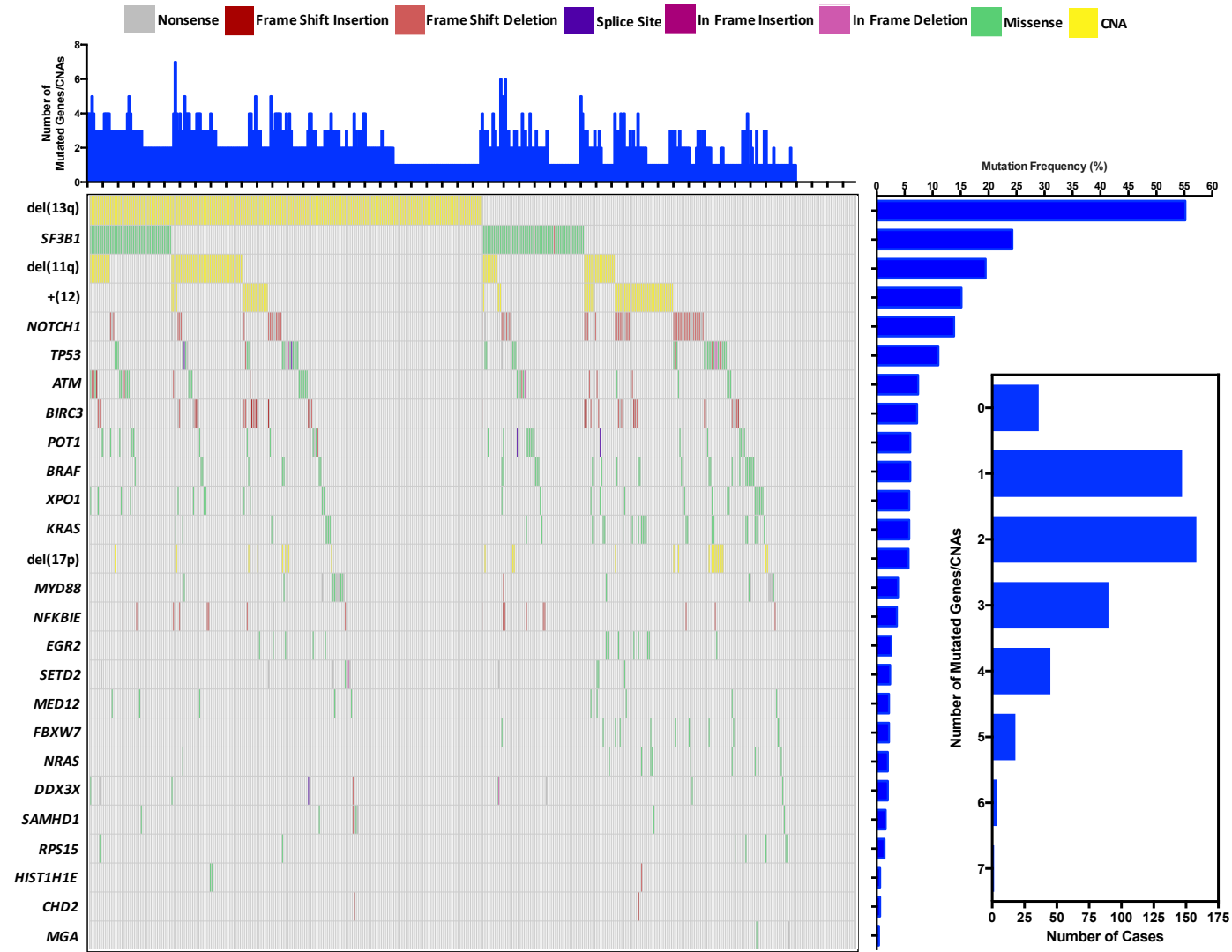
Variable	Status	Overall Survival									Progression-Free Survival								
		Total	Events	Median (years)	LCI	UCI	HR	LCI	UCI	P Value	Total	Events	Median (years)	LCI	UCI	HR	LCI	UCI	P Value
<b>BRAF</b>	Unmutated	469	383	6	5.39	6.55	-	-	-	-	469	429	2	1.83	2.33	-	-	-	-
	Mutated	30	28	2.87	6.25	7.5	1.66	1.13	2.44	0.009	30	30	2.12	1.42	3.33	1.11	0.77	1.61	0.586
<b>EGR2</b>	Unmutated	486	398	5.95	5.08	6.39	-	-	-	-	486	446	2.08	22	28	-	-	-	-
	Mutated	13	13	3.45	3.85	-	2.91	1.67	5.1	<0.0001	13	13	0.415	10	NA	2	1.15	3.49	0.012
<b>KRAS</b>	Unmutated	470	383	5.89	5.32	6.44	-	-	-	-	470	430	2.04	22	28	-	-	-	-
	Mutated	29	28	3.83	2.79	6.86	1.96	1.33	2.89	<0.001	29	29	1.92	18	35	1.29	0.89	1.89	0.18
<b>MYD88</b>	Unmutated	480	401	5.67	4.96	6.25	-	-	-	-	480	442	1.96	21	27	-	-	-	-
	Mutated	19	10	10.3	7.15	-	0.42	0.22	0.79	0.005	19	17	2.67	27	68	0.76	0.47	1.23	0.262
<b>NFKBIE</b>	Unmutated	481	393	5.9	5.32	6.47	-	-	-	-	481	441	2	22	28	-	-	-	-
	Mutated	18	18	3.61	2.77	6.98	2.01	1.25	3.23	0.003	18	18	1.83	16	35	1.59	0.99	2.55	0.054
<b>NOTCH1+3'UTR</b>	Unmutated	375	306	6.22	5.56	6.73	-	-	-	-	430	391	2.17	22	28	-	-	-	-
	Mutated	69	62	4.28	3.62	6.03	1.47	1.12	1.94	0.005	69	68	1.92	17	30	1.24	0.96	1.61	0.099
<b>NRAS</b>	Unmutated	489	401	5.88	5.23	6.44	-	-	-	-	489	450	2	22	28	-	-	-	-
	Mutated	10	10	4.24	2.05	-	2.21	1.18	4.16	0.011	10	9	2.54	19	NA	0.9	0.47	1.75	0.758
<b>RPS15</b>	Unmutated	492	404	5.86	5.3	6.42	-	-	-	-	492	452	2.08	22	28	-	-	-	-
	Mutated	7	7	2.89	2.18	-	2.37	1.12	5.03	0.02	7	7	1.75	3	NA	1.99	0.94	4.21	0.067
<b>SF3B1</b>	Unmutated	378	301	6.33	5.64	6.99	-	-	-	-	378	344	2.17	22	29	-	-	-	-
	Mutated	121	110	4.49	3.92	5.65	1.48	1.19	1.85	<0.001	121	115	1.92	17	28	1.19	0.96	1.47	0.112
<b>TP53</b>	Unmutated	444	360	6.15	5.64	6.7	-	-	-	-	451	413	2.17	23	29	-	-	-	-
	Mutated	55	51	2.65	1.47	3.87	2	1.49	2.69	<0.001	48	46	0.5	5	15	1.95	1.27	2.34	<0.0001

**Table 2. Multivariate Cox model for overall survival and progression free survival in CLL4.**

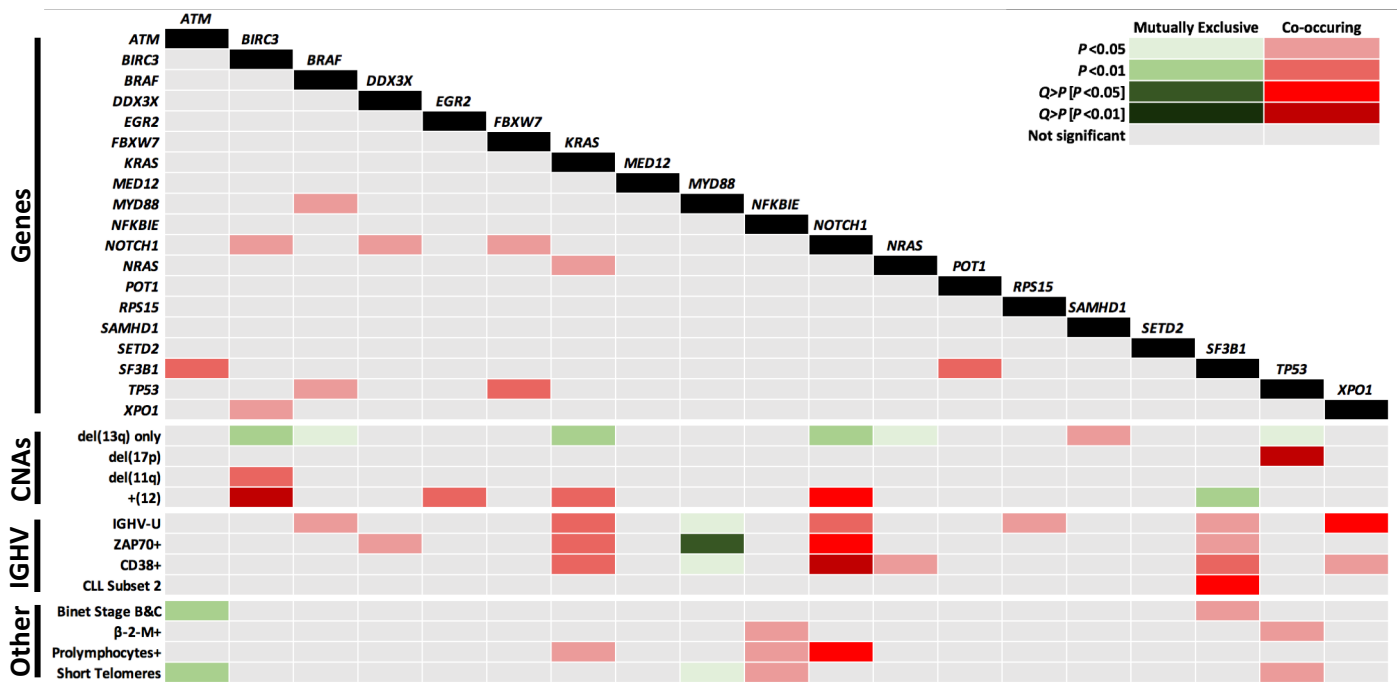
Survival	Variable	HR	LCI	UCI	<i>P</i>
Overall	<b><i>TP53ab</i></b>	4.247	2.932	6.151	<0.0001
	<b>Biallelic <i>BIRC3</i></b>	2.756	1.397	5.438	0.003
	<b><i>EGR2</i> mutated</b>	2.188	1.167	4.099	0.015
	<b>IGHV-U</b>	1.831	1.417	2.364	<0.0001
	<b><i>MAPK-ERK</i> mutated</b>	1.683	1.202	2.356	0.002
	<b><i>SF3B1</i> mutated</b>	1.544	1.191	2.002	0.001
	<b>Binet Stage B &amp; C</b>	1.454	1.102	1.918	0.008
	<b>11q deletion</b>	1.431	1.081	1.895	0.012
Progression-Free	<b><i>TP53ab</i></b>	4.975	3.049	8.118	<0.001
	<b>Short Telomeres</b>	1.964	1.466	2.629	<0.001
	<b>11q deletion</b>	1.816	1.226	2.688	0.003
	<b>Biallelic <i>BIRC3</i></b>	3.833	1.537	9.557	0.004
	<b>Prolymphocytes</b>	1.508	1.034	2.198	0.033

The OS model was built using the following starting variables: *MAPK-ERK*mut, *TP53ab* (after removal of <12% *TP53* mutations), *EGR2*mut, *RPS15*mut, *NFKB1*Emut, *MYD88*mut, *SF3B1*mut, *NOTCH1*+3'UTRmut, Binet Stage B&C, 11q deletion, biallelic *ATM*, biallelic *BIRC3*, sole 13q deletion, trisomy 12, IGHV-U. The final model for OS consisted of 391 patients and 323 events. The PFS model was built using the following starting variables: *TP53ab*, *EGR2*mut, biallelic *ATM*, biallelic *BIRC3*, 11q deletion without *ATM* or *BIRC3* mutations, sole 13q deletion, Short Telomeres, Prolymphocytes+, and IGHV-U. The final model for PFS consisted of 225 patients and 210 events. Variables for both OS and PFS MVA models were removed using the backwards selection method. HR = Hazard Ratio, LCI = Lower Confidence Interval, UCI = Upper Confidence Interval, *P* = Multivariate Log Rank *P* value.

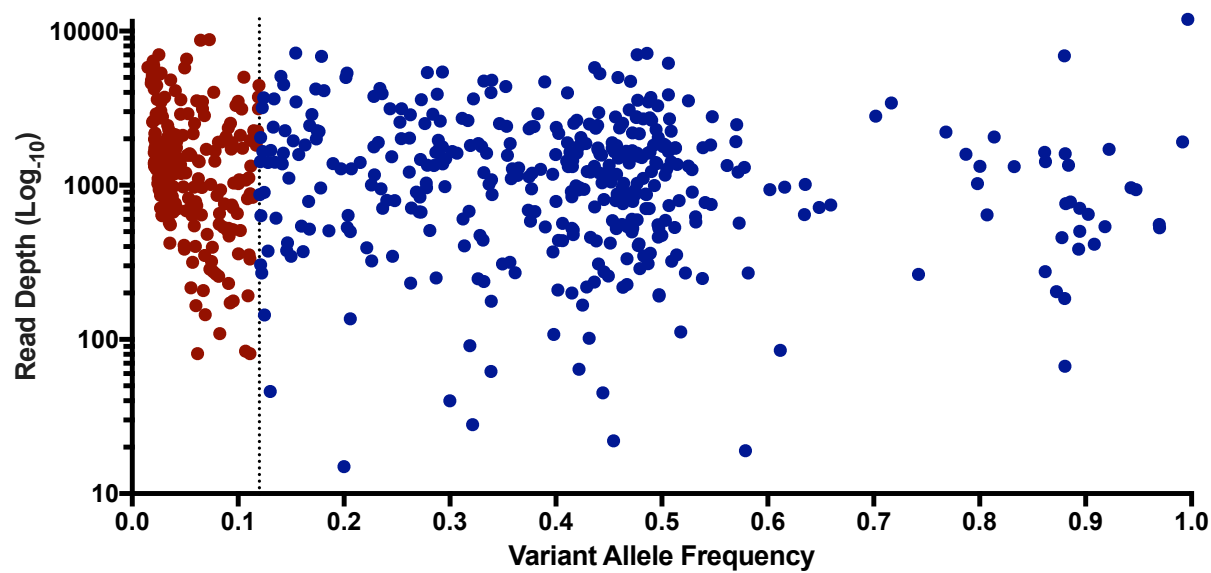
A



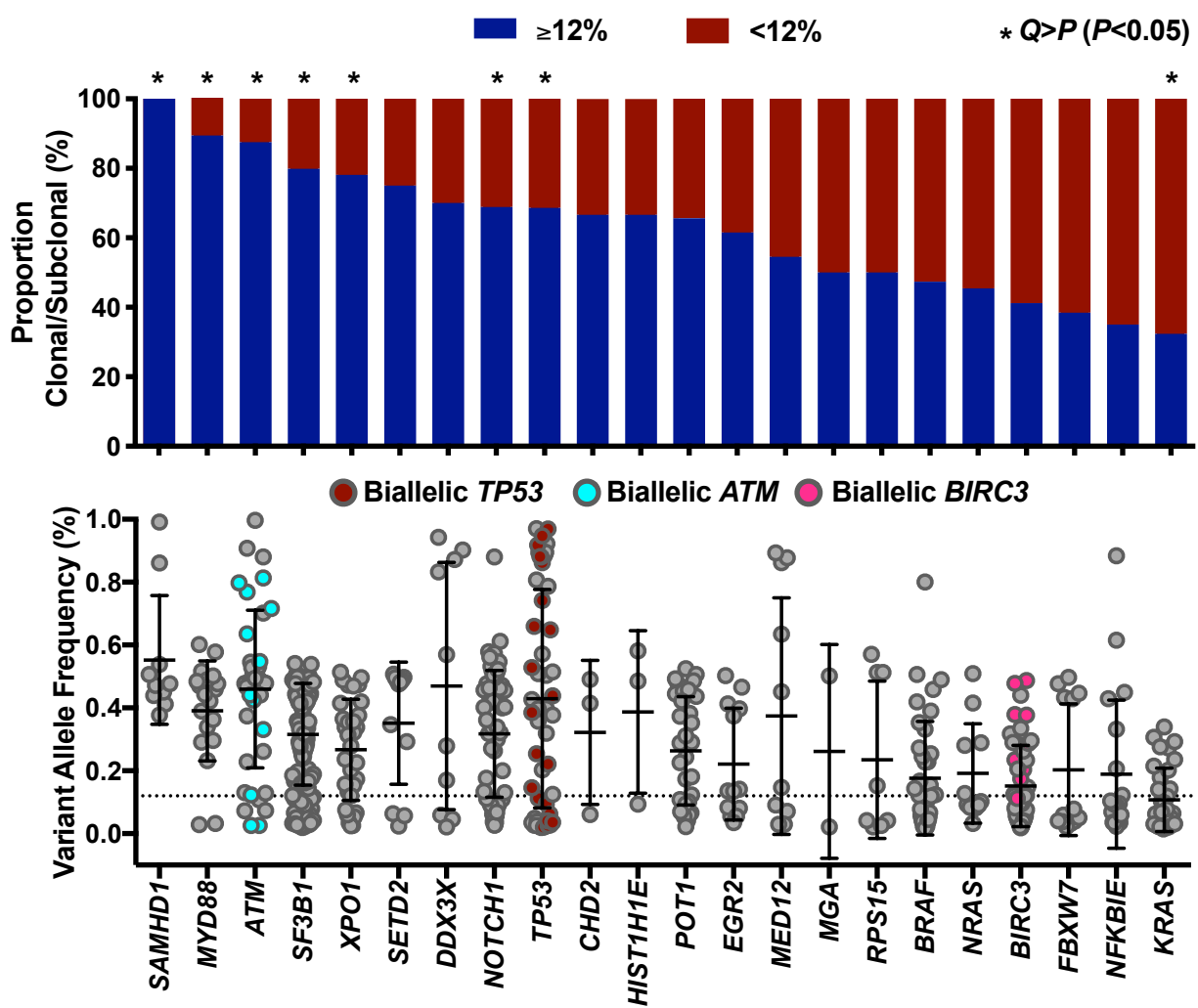
B

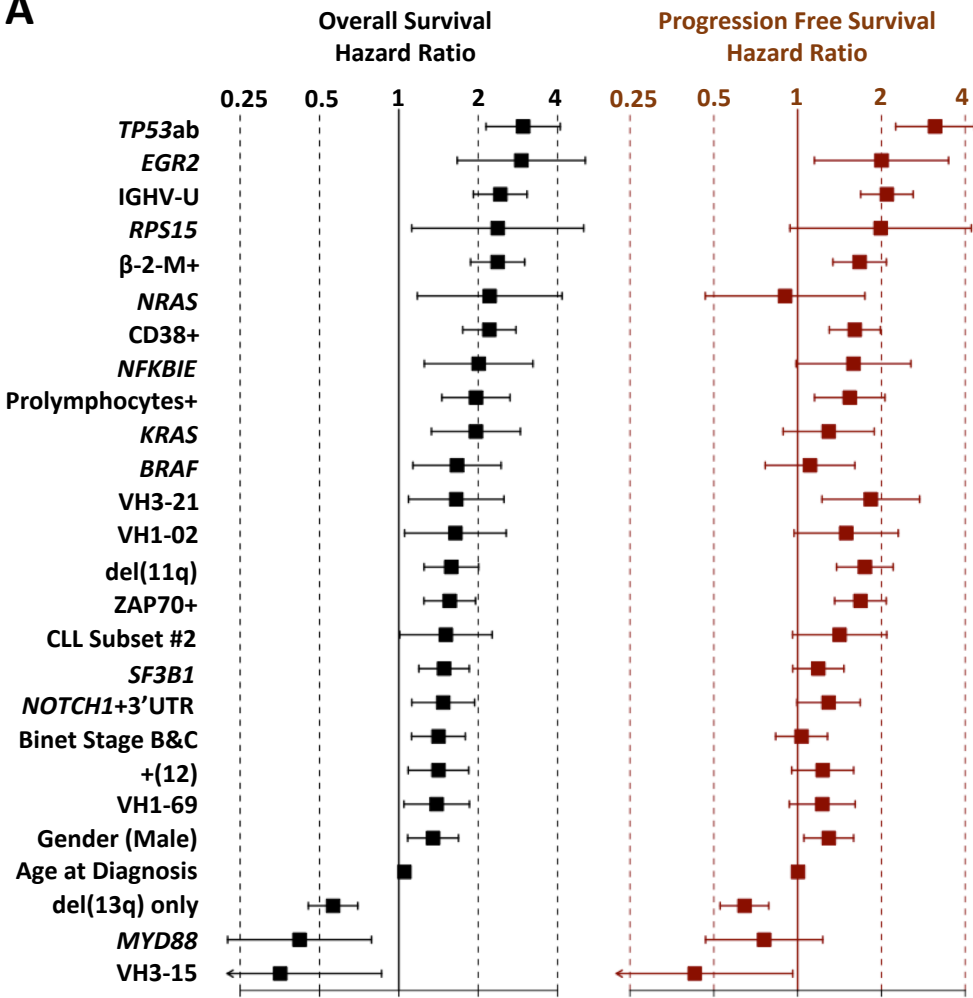
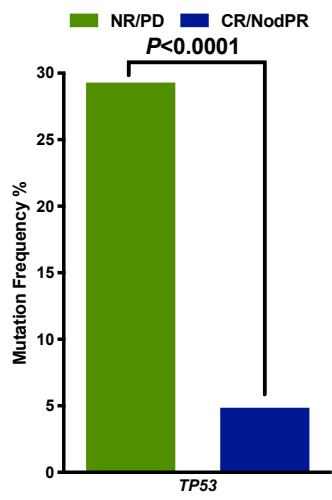
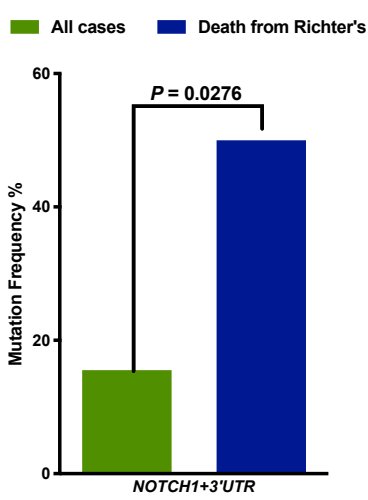
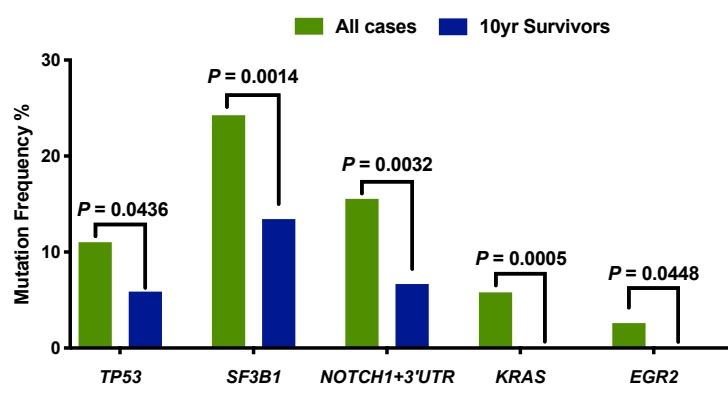


A



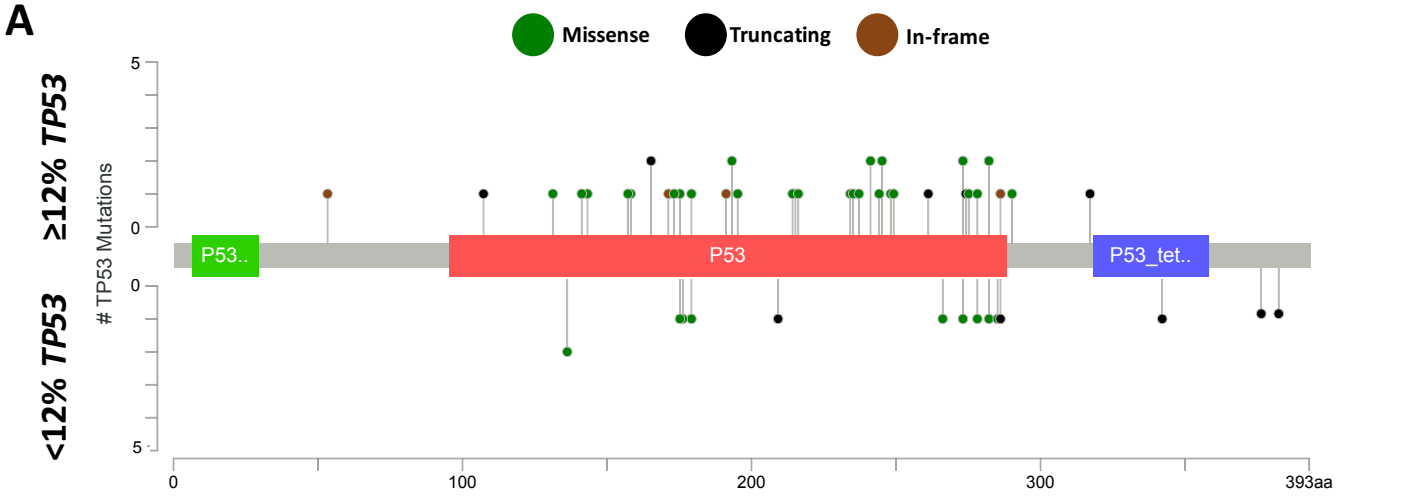
B



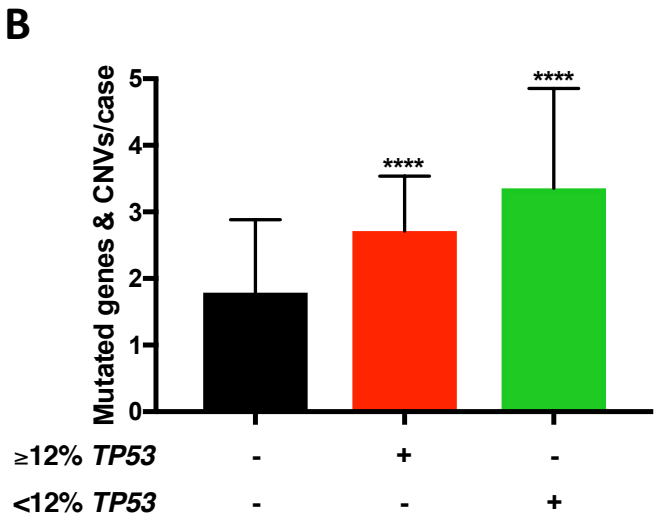
**A****B****C****D**



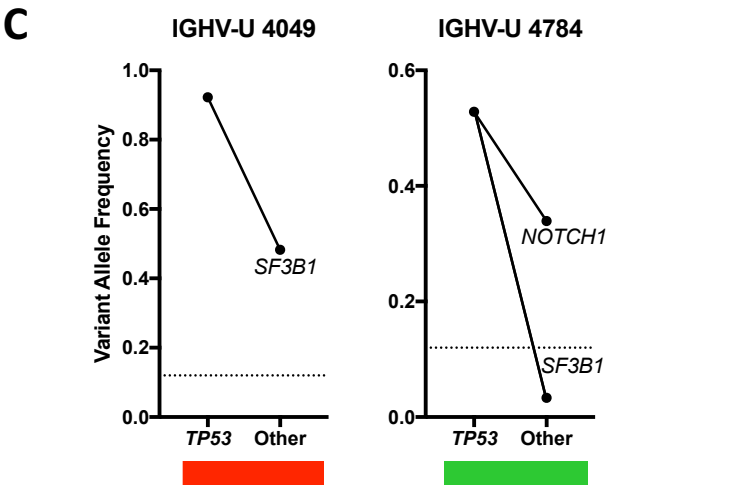
A



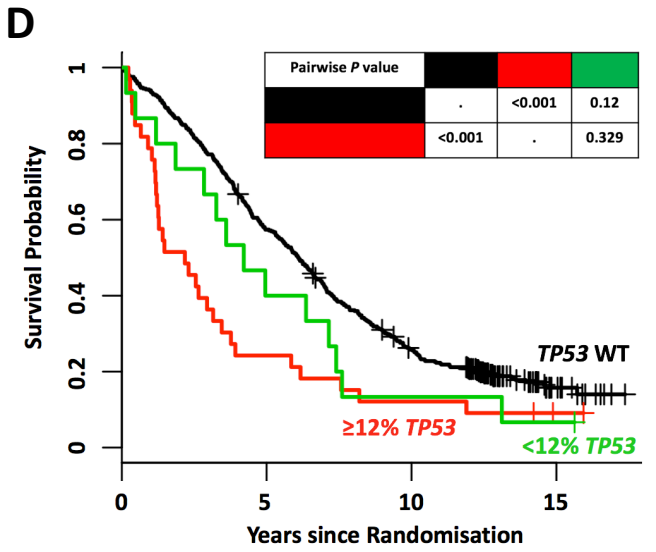
B



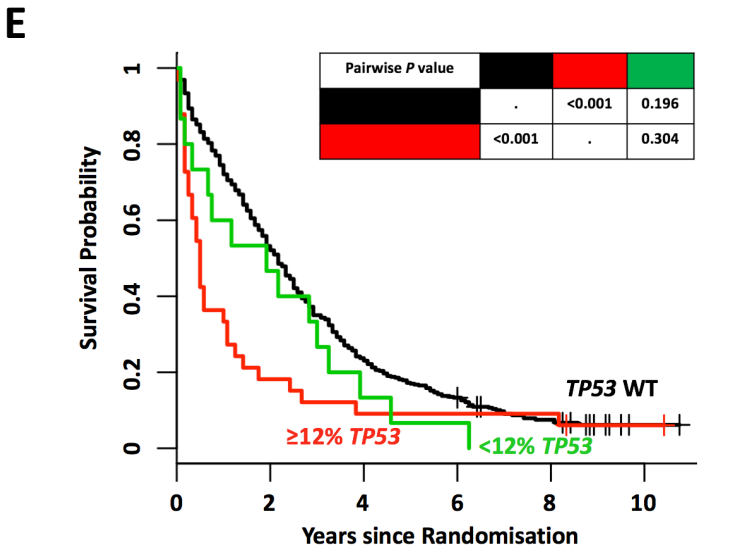
C

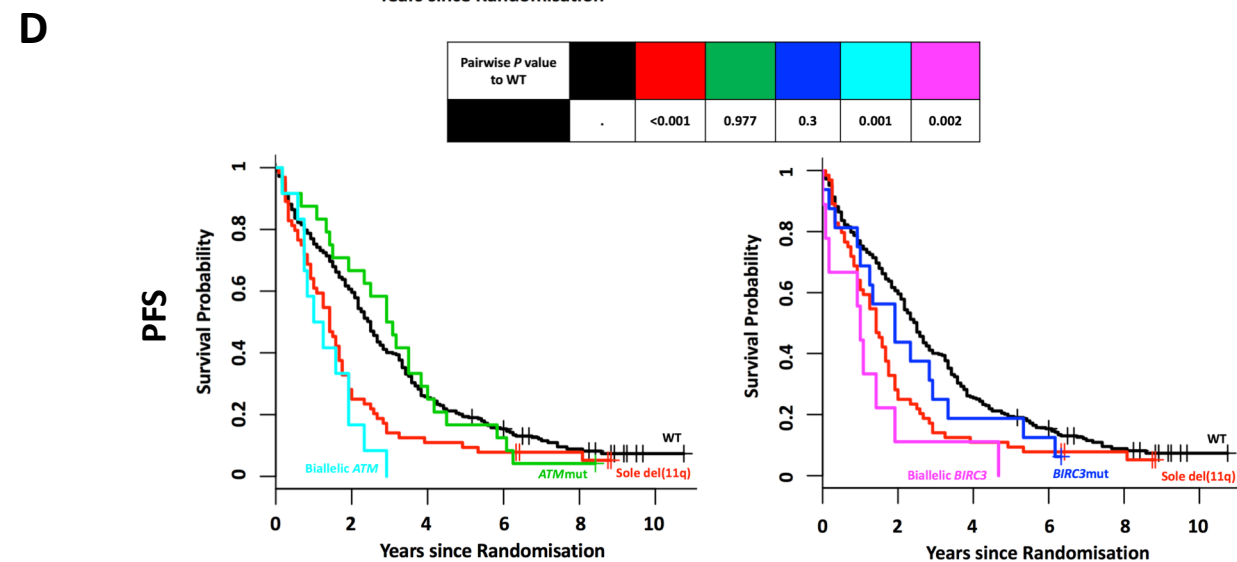
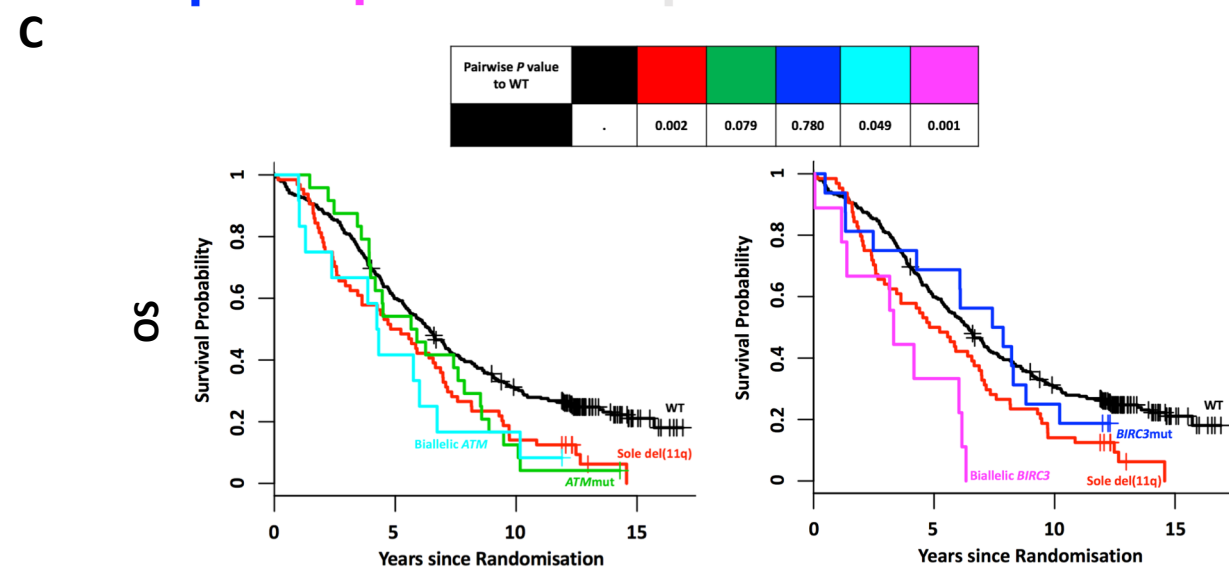
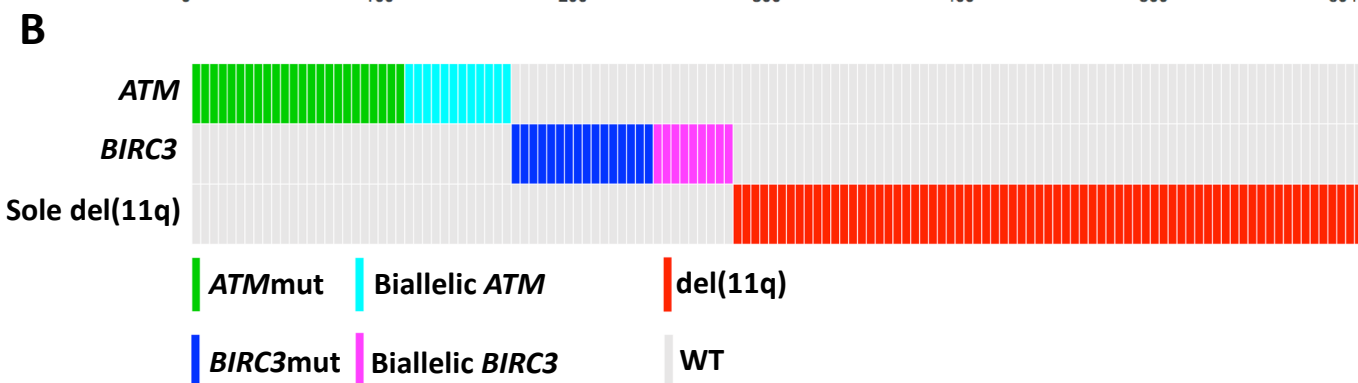
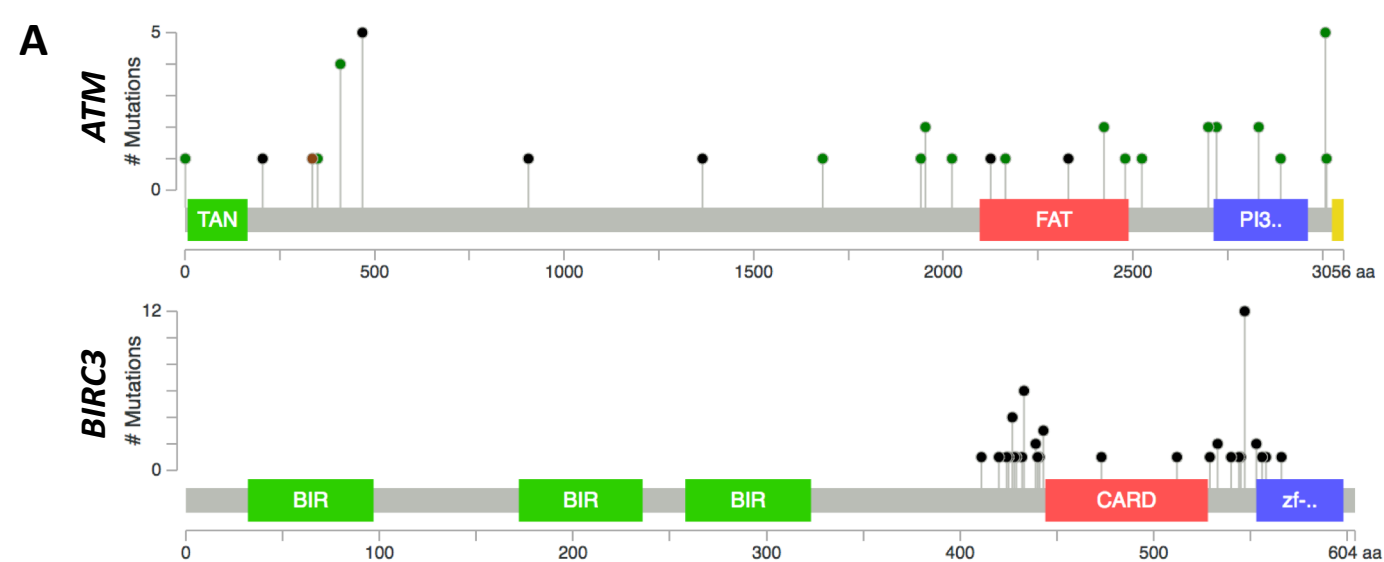


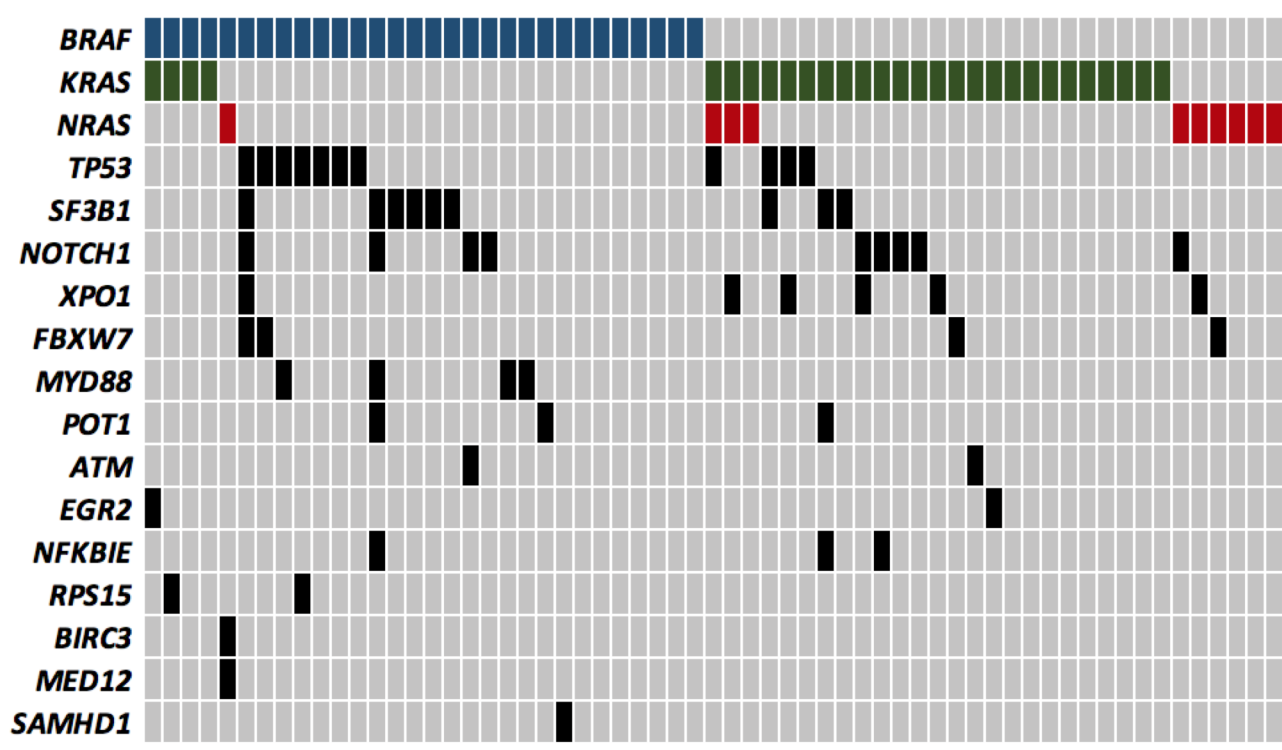
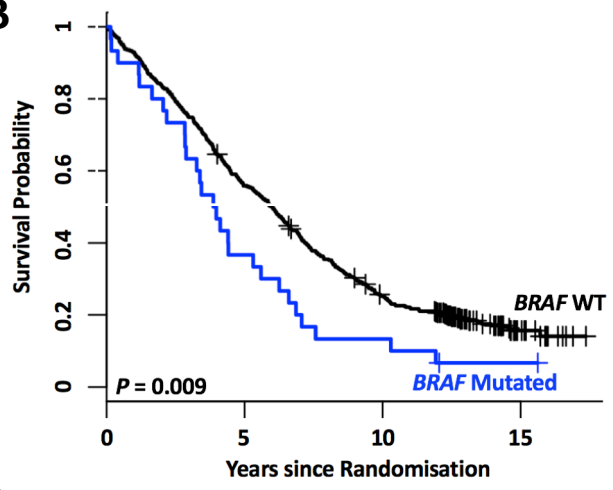
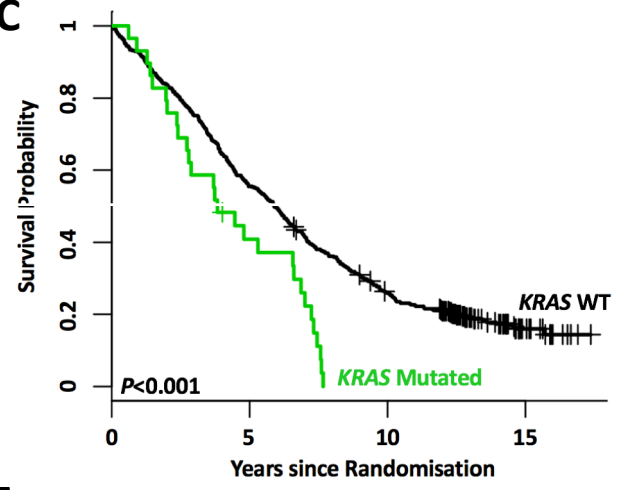
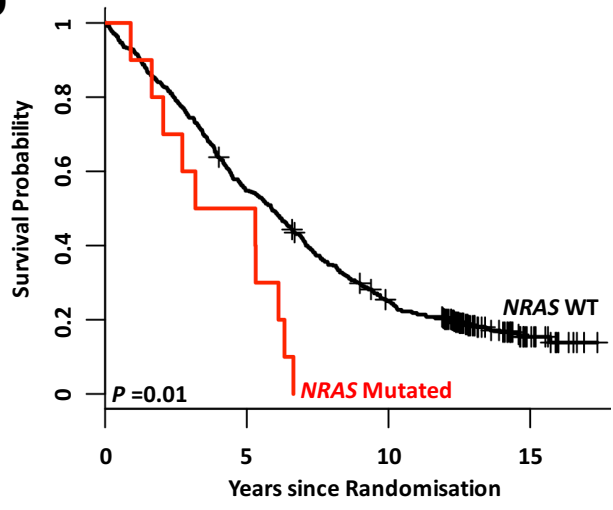
D



E





**A****B****C****D****E**